J Petrol Explor Prod Technol (2017) 7:1095–1112
DOI 10.1007/s13202-017-0324-4

ORIGINAL PAPER - PRODUCTION ENGINEERING

Modeling and simulation of gas flow behavior in shale reservoirs

Vamsi Krishna Kudapa[1] · Pushpa Sharma[1] · Vibhor Kunal[1] · D. K. Gupta[1]

Received: 6 September 2016 / Accepted: 5 January 2017 / Published online: 2 February 2017

Abstract Shale is a growing prospect in this world with decreasing conventional sources of fossil fuel. With the growth in demand for natural gas, there is impending need for the development of the robust model for the flow of shale gas (Behar and Vandenbroucke in Org Geochem, 11:15–24, 1987). So the major driving force behind the working on this major project is the unavailability of desired models that could lead to enhanced production of these wells and that too efficiently. This model mainly includes the movement of shale gas from tight reservoir through the conductive fractures to wellbore and production model of the decline in pressure inside the reservoir with respect to time. This result has been further compared with the help of MATLAB so as to obtain a complete pressure-derived model. The result shows the applicability of this in the real-life projects where it is difficult to model the fractures and obtain the flow rate with them in fractures and how to set the production facilities becomes a question.

Keywords Shale · Shale gas · Desorbed gas · Adsorbed gas · MATLAB · CMG-IMEX simulator

Introduction

Shale is known as fine-grained, clastic sedimentary rock. The molecule size of shale is little which makes the interstitial spaces likewise little. Indeed, they are minute to the point that oil, regular gas and water experience issues traveling through the development. Shale can hence serve as a compelling top rock for oil and common gas (Firoozabadi 2012). Despite the fact that the interstitial spaces in shale are minute, they can take up a huge volume of the arrangement rock. This lets the shale to hold noteworthy measures of water, gas or oil and not have the capacity to adequately transmit them as a result of its low permeability. The petroleum business has beat these confinements of shale developments by utilizing level penetrating and hydraulic cracking to make build porosity and permeability inside the stone (Bustin et al. 2008).

Shale gas will be gas that is actually present in shale rocks. Sandstone rocks are known for high permeability, and gas can stream effortlessly through the stone. Interestingly, shale shakes for the most part have low permeability (Bustin et al. 2008).

Shale gas is viewed as an alleged "unusual gas," together with "tight gas" with low permeability and "coal-bed methane" (CBM). While both traditional and capricious stores contain normal gas, it is the more intricate generation strategies that recognize the ordinary and offbeat store (Gong et al. 2011). Hydraulic breaking is regularly connected to capricious normal gas stores. India has immense stores of shale gas. As indicated by the accessible sources, India has around 300–2100 tcf evaluated gas setup in Indian shale gas bowls which is much bigger than stores that are accessible in Krishna–Godavari (D 6) Basin (Swami et al. 2013).

This paper mainly discusses about the modeling of gas flow from the matrix to the wellbore. The representation of the reservoir model includes a cube as a porous media, i.e., it contains pore spaces in which free gas is stored and also the adsorbed gas. Now, the gas in the cube (both free gas and adsorbed gas) will start flowing out inside the matrix to the fractures (induced). Many of these cube representations are put together and connected to the well bore.

✉ Vamsi Krishna Kudapa
vamsikrishna234353@gmail.com

[1] Petroleum Engineering Department, University of Petroleum and Energy Studies, Dehradun, India

In this paper, we have considered a updated dual-mechanism model. One porosity is the combination of matrix and natural fracture, and the second porosity is the hydraulic fracture. For this model, a nonlinear PDE equation has been developed which is then compiled using MATLAB to develop a simulator for calculating the shale gas production, by considering the matrix as a source term. The production data that are obtained from this model will describe the unique characteristics shale gas reservoirs.

A three-dimensional shale gas reservoir model was created. Three flow mechanisms (Darcy flow and non-Darcy flow) as well as gas adsorption and desorption mechanism were considered in this model. The flow in the matrix is considered as single-phase flow, and the production from this reservoir model is estimated for a period of 3 years and the results are validated by CMG-IMEX software.

Back ground literature

Modeling of unconventional gas reservoirs and its application for determining pressure variations and estimating production rate are carrying on for the past many years and are generally classified as numerical or analytical methods. Transport of shale gas in the reservoirs is a complex multi-scale transport process, which is from hydraulic fractures, i.e., macropores to the natural fractures, i.e., micropores (Javadpour et al. 2007a, b). Lots of researches have been done on transport mechanism of shale gas from matrix pores to the fractures. In general, most of the authors believe that the flow of gas in the fractures will follow Darcy's Law, but the flow behavior of gas in matrix pores is still controversial. Zuber et al. (2002), Schepers et al. (2009), Wang and Reed (2009), Song and Ehlig-Economides (2011) and Song (Song and Yang 2013) conducted several studies and proposed that the flow of gas from the matrix pores to the fractures in shale gas reservoirs follows Darcy's law. Rushing et al. (1989), Dahaghi (2010) and Dahaghi and Mohaghesh (2011) have proposed that the flow of gas from the matrix pores to the fracture network is by diffusion. Javadpour (2009) and Ozkan et al. (2010) state that the flow and diffusion take place at the same time when the gas migrates from matrix pores to fracture network. As the permeability of the reservoir varies with location, it is not possible to have a unique permeability for the entire reservoir. For representing a uniform permeability for shale gas reservoirs, several investigations were performed on apparent gas permeability for representing the gas flow in shale reservoirs. Several investigations on apparent gas permeability have been done for representing the flow of gas in the nanopores (Clarkson and Nobakht 2011, Clarkson et al. 2012a, Clarkson and Williams 2012b; Michel et al. 2011; Civan et al. 2011; Sakhaee-Pour and Bryant 2012; Javadpour et al. 2007a, b; Javadpour 2009; Swami et al. 2012, Swami et al. 2013; Fathi et al. 2012).

One of the major factors in determining the productivity index of the shale gas reservoir depends upon the fracture network (Brown et al. 2009). In general, all the fractures are sourced by the matrix system. In most of the cases, a question arises about the contribution of shale matrix system to the fracture system. Unfortunately, with the available research a complete understanding of fluid transfer from shale matrix to fracture network is unknown. The present studies revealed that the main contributor to the flow of gas in the matrix is Darcy's flow, which is induced due to pressure differential between the matrix and the fracture. Many authors have made different assumptions regarding the flow of gas in the shale matrix, as the fundamental assumption of Darcy's flow in shale matrix revealed that the gas flow in the nanopores is considered negligible (Ozkan et al. 2010). In oder to have a clear idea about the flow of gas in the shale matrix, a detailed research has to be done.

Recently, Javadpour et al. 2007a, b; Javadpour 2009 described the flow in shale matrix by Knudsen diffusion and slip flow in nanopores, Darcy's flow in the micropores, desorption from surface of the kerogen and the diffusion from the surface of the solid kerogen. Our objective in this paper is to include more detailed description of flow in shale matrix to the modeling of production from the fractured shale gas reservoir. Here, we limit our focus on Darcy's flow, non-Darcy's flow and desorption flow process. Desorption of gas in shale reservoirs has been linked to the coal-bed methane reservoirs where gas desorbs from the surface of the coal matrix block to the cleats (Induced Fractures). In shale gas reservoirs, the gas will be stored in the form of free gas and the adsorbed gas.

Here, we are presenting an updated dual-mechanism dual-porosity that accounts the free gas in the reservoir pores and the adsorbed gas on the surface of the kerogen. We consider a cubical matrix blocks, which consists of free gas and the adsorbed gas. As the pore space in the matrix reduces due to pressure reduction in the reservoir, the compressibility of the reservoir is also considered. The general formulation presented here represents the flow of gas in the matrix. The reservoir is divided into 5*5*5 matrix blocks. Now, mass balance equation is developed by considering a unique matrix block in the reservoir.

Benefits

Shale gas is connected with significantly less carbon emissions as compared to coal. It can also decrease energy costs because huge amount of shale gas production would likely cause a decline in the price of natural gas. High shale gas production would also help our energy security and reduce our dependence on foreign fossil fuels (Ding et al. 2011). Shale gas could also provide better and cleaner energy

option for many developing countries that are currently dependent on coal which is the dirtiest energy source.

Risks

There are additionally some disservices of shale gas. Shale gas, in spite of being essentially cleaner vitality source when contrasted with coal, regardless frees noteworthy carbon outflows, in this way being less satisfactory from ecological perspective than renewable wellsprings of vitality (Hong et al. 2013). Additionally, ecological danger as potential spillages of methane gas from different wells of shale gas could balance the decrease of carbon dioxide and atmosphere advantage of changing from coal to shale gas. The fast improvement in shale gas businesses could back off the advancement of renewable vitality, particularly if shale gas gets to be one of the least expensive vitality choices accessible. Renewable vitality is thinking that it is hard to contend with coal, and with modest and effectively accessible shale gas, things could turn out to be much more terrible for the area of renewable vitality. Right now, the removing expense of shale gas is higher when contrasted with the expenses of extraction of routine gas or coal; however, the up-and-coming upgrades in boring innovations could diminish the extraction costs (Alahmadi 2010).

Methodology

In the process of fluid flow characterization in shale reservoir, two basic approaches were used. The basic and initial approach is developing nonlinear partial differential equations which represent the flow of gas in the matrix and the flow of gas in the induced fractures and compiling these equations in MATLAB.

A second approach of solving and obtaining all the parameters will be used by the help of simulators. For the matter of credibility, the result of the equations derived from the first approach which are solved in MATLAB will be cross-checked with the results of the second approach using CMG-IMEX reservoir simulator.

Approach by MATLAB

MATLAB is used in our project to solve number of partial differential equations. The set of partial differential equations are solved by finite difference method by assuming some of the constants using the standard literature (Zhang and Yuan 2002). A generic equation is simplified which will change according to reservoir matrix in three dimensions by variables which are *(i, j, k)* which vary according to *(x, y, z)*. The number of equations formed will depend on dimensions of the number of matrix assumed; for example, for $n = 5$, number of equations formed will be $5*5*5 = 125$ equations. These equations are solved by using a MATLAB code using functions of matrices.

The following is the list of variables that are used in the code which can be later changed of different conditions:

- *Pm*–For initial reservoir pressure.
- *T*–For total number of days.
- *Dt*–For time period.
- *dx, dy, dz*–For reservoir length, breadth and depth.
- *N*–For number of Matrix we want to solve.

A number of functions are created to facilitate the calculation of constants with respect to pressure changes at each reservoir point and with respect to time.

A nested loop is used to run the solution code by assigning the constants of each equation in a 3-D matrix and solving it for the values of the variables (Daniel Arthur and Coughlin 2012). A level 5 nesting codes are used in our coding. The final solution matrix is displayed using four-dimensional matrix for every time step.

Code description

The complete code is attached with Appendix 1.

The motive of this code is to solve a generalized linear equation for pressure values at each point in the given matrix. The number of unknown variables in the given matrix depends on the order of matrix assumed; for example, if we assume a matrix of the order of $[5 \times 5 \times 5]$, then the number of elements in the given matrix will be 125, which further means that the number of unknown pressure points to be calculated by the generalized equation assumed previously would be 125.

The matrix that is considered in the project is in accordance with the dimensions of the physical shale rock matrix with following dimensions:

- Length = 22ft.
- Height = 12ft.
- Thickness = 2ft.

To perform a solution for linear equations with such a large number of values, a generalized code is prepared which can be easily modified and used for different values for order of matrix, initial pressure and other different dependent variables.

The generic equation that was derived was a linear equation with seven unknown variables. A particular set of these unknown variables is unique for every point in the matrix. In this way by employing an equation for every point and calculating the corresponding seven unknown variables, pressure difference value at every point in the given matrix can be found for a particular value of time (Dreier 2004).

This step is repeated for every time interval for the complete duration of the project life or the well production

period of the shale reservoir. The value of time interval and the complete duration of the project life are assumed as follows:

- Time interval (dT): 10 days.
- Time duration (T): 1000 days.
- Number iterations done: 100.

The equation along with the seven unknown variables has their corresponding coefficients and a single constant value at the right-hand side of every equation. The value of these coefficients and constants depends on the pressure values of the matrix of the preceding time interval. These coefficients and constants change at each point in the matrix and with each time step. At the initial time, i.e., at $t = 0$, governing factor for these coefficients and constants is the initial pressure value. As the time changes, i.e., at the second time step the value of these will be depending on the previous pressure value at the respective point. So these coefficients and the constants are made dynamic whose values are getting updated with each successive iteration. A code snippet is attached (Fig. 1).

Dynamic updating of coefficients and constants

The complete set of the equations, i.e., 125 equations, are solved using the standard matrix analogy. Every coefficient and constant of matrix are identified with the help of index position which corresponds to each point in the matrix as discussed above. All these equations are first arranged in a standard form and the left-hand side, i.e., the coefficient values are stored in a newly defined two-dimensional matrix, with every row containing the coefficients of that particular equation columnwise. The right-hand sides of the equations, i.e., the constants, are stored in the form of a single column matrix. This is done by using the following code (Fig. 2).

These set of matrices are then solved by the standard matrix form, i.e., $AX = B$. The inverse of the two-dimensional matrix is calculated and multiplied by the single column matrix to achieve 125 pressure values which are also in the form of a single column matrix. These single column matrixes with 125 fresh calculated values are then assigned to their respective places in the matrix using the technique of index assignment casting. This complete technique is shown in the following snippet (Fig. 3).

In the end, a 4-D matrix is considered with the fourth order to be made equal to the number of time steps, at which each set of 3-D matrices containing the pressure values is stored.

NOTE: The complete code of the project is attached with Appendices 1 and 2.

Approach by CMG-IMEX simulator

In this, we are going to present the approach for preparing the flow model by the help of validation software for simulation of CMG-IMEX simulator (Li 2007). This is a unique in its kind of software for showing the shale gas simulation at various points in the grid blocks.

The methodology basically involves of following steps to perform the analysis:

1. I/O Control
2. Reservoir
3. Components
4. Rock fluid
5. Initial conditions

```
122 -     for i=1:n
123 -     for j=1:n
124 -     for k=1:n
125
126 -         Km=klinkenberg( P(i,j,k,y) );
127 -         Tgsc = trans( P(i,j,k,y) );
128
129 -         B(i,j,k)= (Km * Az*Tgsc)/dz;
130 -         S(i,j,k)= (Km * Ay*Tgsc)/dy;
131 -         W(i,j,k)= (Km * Ax*Tgsc)/dx;
132 -         E(i,j,k)= (Km * Ax*Tgsc)/dx;
133 -         N(i,j,k)= (Km * Ay*Tgsc)/dy;
134 -         A(i,j,k)= (Km * Az*Tgsc)/dz;
135
136 -         X(i,j,k)= ((-1)*(dx*dy*dz)/dt)*((Sgm*mat_por(P(i,j,k,y))*cmprs(P(i
137 -         Q(i,j,k) = -1*X(i,j,k)*P(i,j,k,y);
138 -         C(i,j,k) = (E(i,j,k)+W(i,j,k)+N(i,j,k)+S(i,j,k)+A(i,j,k)+B(i,j,k)-
139
140 -     end
141 -     end
142 -     end
```

Fig. 1 Snippet showing the calculations of finite difference constants

```
59 -          lun(x,1)=Q(i,j,k);
60 -          temp=(25*(i-1))+(5*(j-1))+k;
61 -          tun(x,temp)= C(i,j,k);
62 -          i1 = i-1;
63 -              if i1>=1
64 -              temp=(25*(i1-1))+(5*(j-1))+k;
65 -              tun(x,temp)=W(i,j,k);
66 -              end
67 -          j1 = j-1;
68 -              if j1>=1
69 -              temp=(25*(i-1))+(5*(j1-1))+k;
70 -              tun(x,temp)=S(i,j,k);
71 -              end
72 -          k1 = k-1;
73 -              if k1>=1
74 -              temp=(25*(i-1))+(5*(j-1))+k1;
75 -              tun(x,temp)=B(i,j,k);
76 -              end
77 -          i1=i+1;
78 -              if i1<=5
79 -              temp=(25*(i1-1))+(5*(j-1))+k;
80 -              tun(x,temp)=E(i,j,k);
81 -              end
82 -          j1=j+1;
83 -              if j1<=5
84 -              temp=(25*(i-1))+(5*(j1-1))+k;
85 -              tun(x,temp)=N(i,j,k);
86 -              end
87 -          k1=k+1;
88 -              if k1<=5
89 -              temp=(25*(i-1))+(5*(j-1))+k1;
90 -              tun(x,temp)=A(i,j,k);
91 -              end
```

Fig. 2 Snippet showing the arrangement of equations in 2-D and column matrix

```
 93
 94 -      sol=tun\lun;
 95
 96 -      for x=1:125
 97 -          [i,j,k]=index(x);
 98 -          dP(i,j,k)=sol(x);
 99 -      end
100
```

Fig. 3 Snippet showing the reverse allocation of pressure values to the original matrix

6. Numerical
7. Wells and recurrent

Reservoir

It is the second type of property set rather the main type of data set which is mainly composed of ten further parameters

1. Grid: involves the following steps to perform the analysis grid type Cartesian–60*60*5 with a dual-porosity model, and the pinch out thickness of 0.0002 is set.
2. Array properties (Figs. 4, 5, 6).
3. Rock fluid properties: default defined values.
4. Sectors: default defined values.
5. Aquifers: no aquifer is potentially used in various models.
6. Lease plane: default defined values.
7. Rock compressibility (Fig. 7).
8. Compaction: default defined Values.
9. Depletion: default defined Values.
10. Flux sectors: default defined values.

These all are the second-step parameter entry into the data set for the purpose of model simulation.

Components

There are lots of properties to be entered into the component section of the simulation work. This work is figuratively the heart of the project with all the data set values from the real-life time scenarios. The component includes various data sets (Fig. 8).

Model

In this section, the model selection, i.e., single-phase or multi-phase flow, is selected and the other properties that related to the gas flow in the reservoir are entered (Fig. 9).

Data set Eg

The image entered below is the graph of the model that is being prepared for the purpose of shale gas evaluation with project-opted values for the shale gas field. Here the entered is between the Eg versus pressure, and the graph is plotted for that (Fig. 10).

The second data set is entered for the properties of Bg versus pressure (psi), and hence, the complete range of graphs that were self-developed was made (Fig. 11).

Rock fluid

In this section, we need to enter the values of the specific parameter of the rock. This is again represented in the form of the graphs which are presented as the snippet below (Fig. 12).

The viscosity properties are also represented in the form of graphs rather than opting for table for the better understanding and illustrative experience; hence, the image describing the gas-phase viscosity change is attached in the form of image (Fig. 13).

Fig. 4 Array properties 1

	Grid Thickness	Porosity	Porosity - Fracture
UNITS:	ft		
SPECIFIED:	X	X	X
HAS VALUES:	X	X	X
Whole Grid	50	0.07	0.03
Layer 1			
Layer 2			
Layer 3			
Layer 4			
Layer 5			

Fig. 5 Array properties 2

Go To Property: Grid Top — Use Regions / Sectors

	Permeability J	Permeability K	Permeability I - Fracture
UNITS:	md	md	md
SPECIFIED:	X	X	X
HAS VALUES:	X	X	X
Whole Grid	0.0001	0.0001	0.01
Layer 1			
Layer 2			
Layer 3			
Layer 4			
Layer 5			

Fig. 6 Array properties 3

Go To Property: Grid Top — Use Regions / Sectors

	Fracture Spacing I	Fracture Spacing J	Fracture Spacing K
UNITS:	ft	ft	ft
SPECIFIED:	X	X	X
HAS VALUES:	X	X	X
Whole Grid	100	50	50
Layer 1			
Layer 2			
Layer 3			
Layer 4			
Layer 5			

The further parameter entry shows the values of the saturation of the liquid and relative permeability which can be found from the reservoir analysis of the particular rock set (Figs. 14, 15).

In the above image, the values changed are for pressure first time step change and the minimum time step. The values for the maximum time step are altered for the best and optimum results.

Wells

In this section, the wells were added and the production time period was selected.So, for the purpose of multiple wells a producer well was drilled into the third layer of the shale gas reservoir.

Horizontal Well—For the creation of horizontal instinct, the well was perforated from the first layer to the third layer, and hence, the well data were taken from the beginning and hence added to the layerwise (Fig. 16).

The data for date and time are attached in the next image which completes the final stepwise methodology (Fig. 17).

Results and discussions

After the complete work, the following results were drawn:

- Pressure profile for a defined region is developed for a certain piece of reservoir zone.

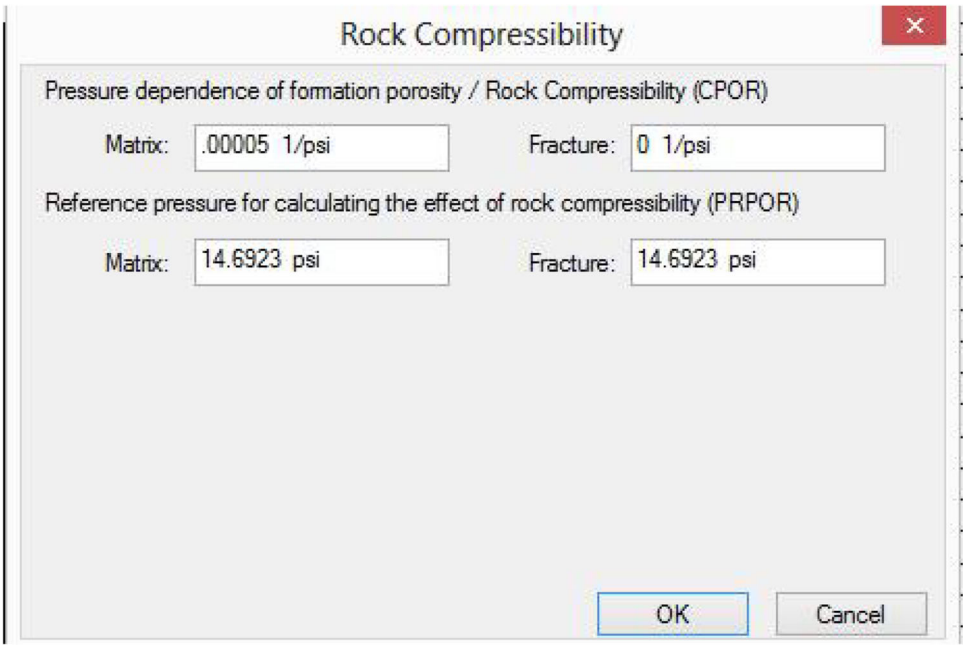

Fig. 7 Values input of rock compressibility

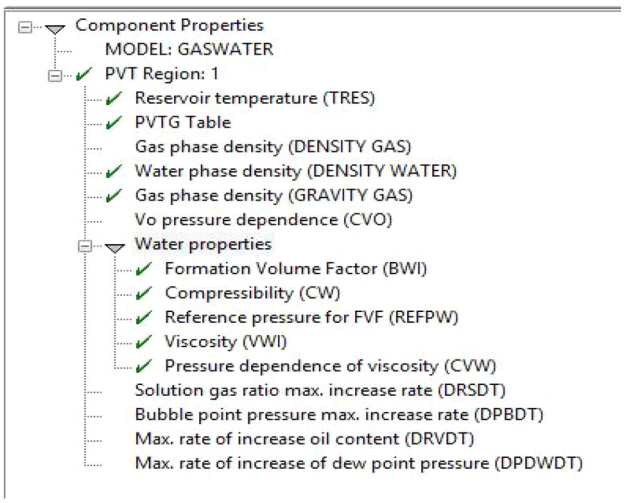

Fig. 8 Different components

- The subsequent models can be prepared using this as a base step for the characterization of fluid from well bore to the surface.

As per the current methodology, the work appears to be promising and will yield a great model of the shale which will be completed from every end and the further study will be revolving around such models which will be founding pillars of the researches.

Our project is stood on mainly two pillars: one pillar is of the MATLAB work for solving the set of nonlinear PDE's and the other pillar is the simulation results. To check the perfection of the developed model, a comparison is done between the two pillars, i.e., the MATLAB results and the CMG-IMEX results.

Our project is stood on four pillars: two mainly inclusive of simulation and the other two of rigorous calculations and MATLAB work.

There is drift from our single goal of developing the pressure transient equations toward multiple goal of multiple application testing and verifying by various means. These already derived variables are sure to yield different values as per different setting in computational methods, but the final result should be in close proximity of what we are trying to achieve and prove by our methods and thus satisfying our far-fetched goals.

Results from MATLAB

The final values obtained from the above code are displayed in the image below. This image shows the various pressure values which are finally obtained and are displayed in the form of a matrix with layer succeeding another layer and finally on a large scale displaying the whole range of pressure values. The initially assumed values were taken and are verified with already available data so that the proper working of the code can be testified.

The pressure depreciation factor can clearly be seen by the values obtained in the form of the four-dimensional matrix. The forth element of the 4-D matrix is utilized to save the matrix in correspondence with the time factor; for each increment in the time interval the pressure values for each matrix are stored in that position in a 3-D form.

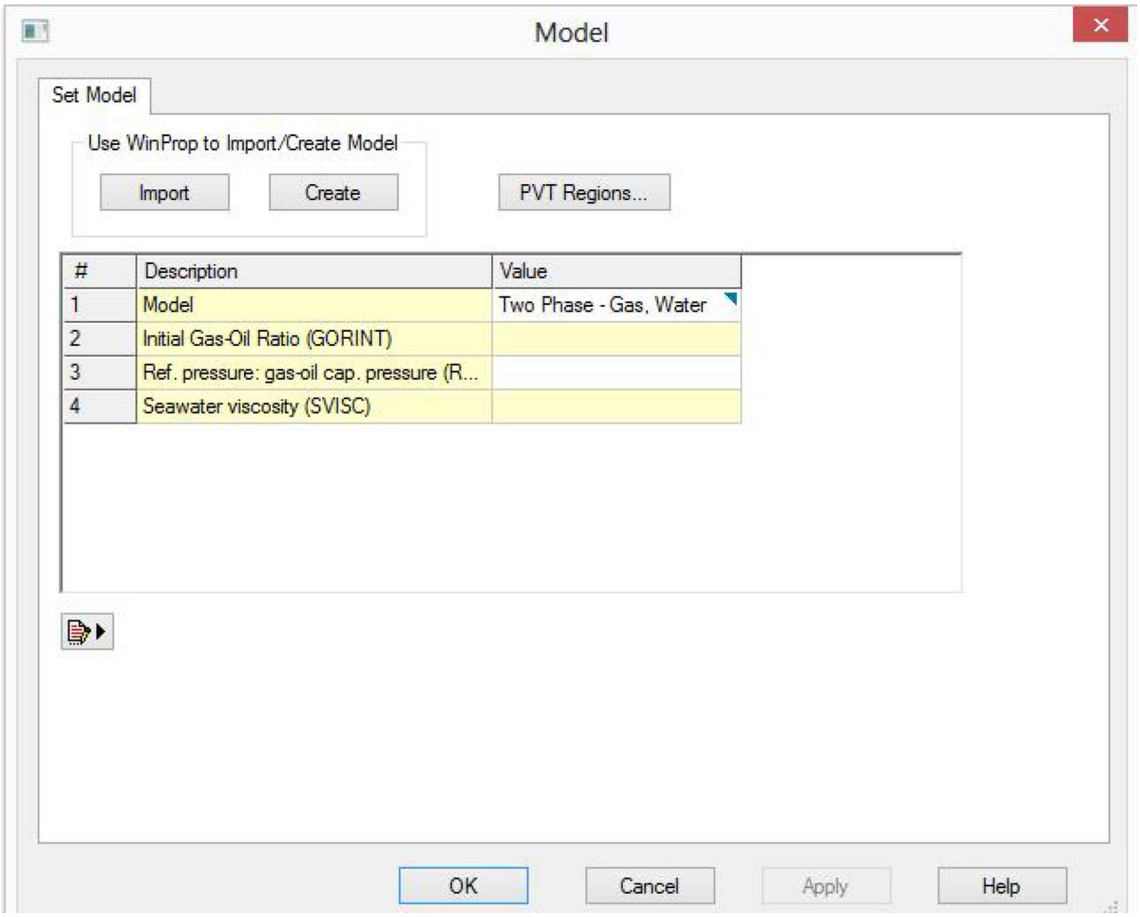

Fig. 9 Model properties

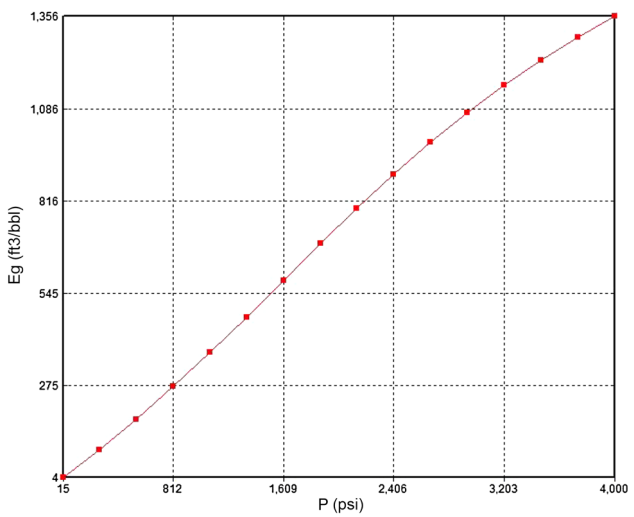

Fig. 10 Eg versus pressure

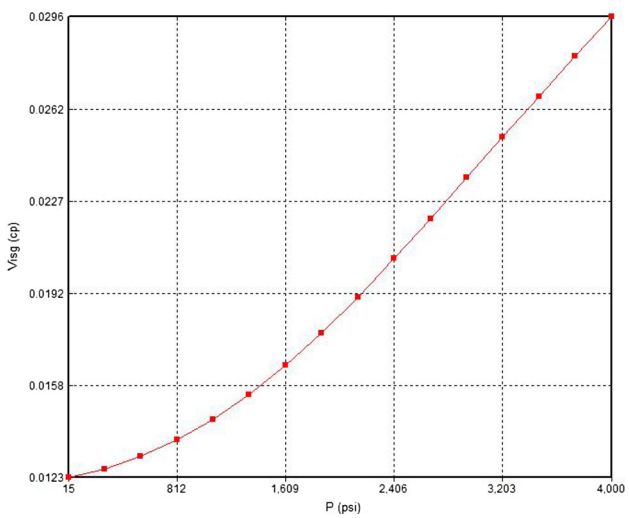

Fig. 11 Formation volume factor (B_b) versus pressure

The depletion of pressure can be clearly depicted from the calculated values. A pattern in the pressure value depletion of the matrix can be clearly seen. In order to get more accurate and clear pressure values and the pattern to study, the time interval between two time steps can be reduced and the order of the matrix can be increased. This would result in more intensive approach to the reservoir pressure values and will provide the pressure values at

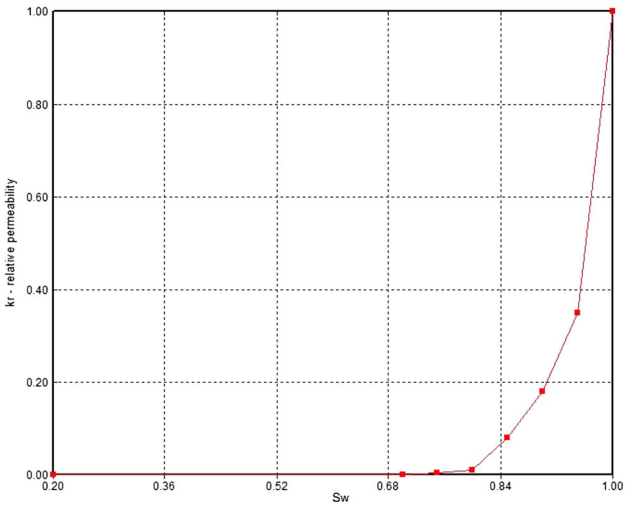

Fig. 12 Relative permeability versus water saturation properties

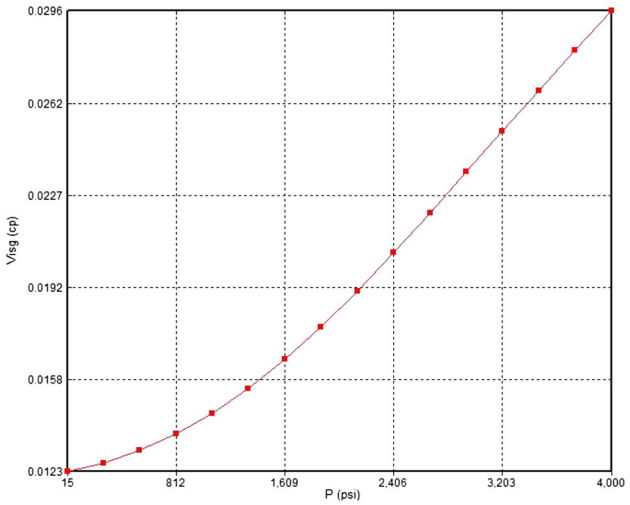

Fig. 13 Viscosity versus pressure

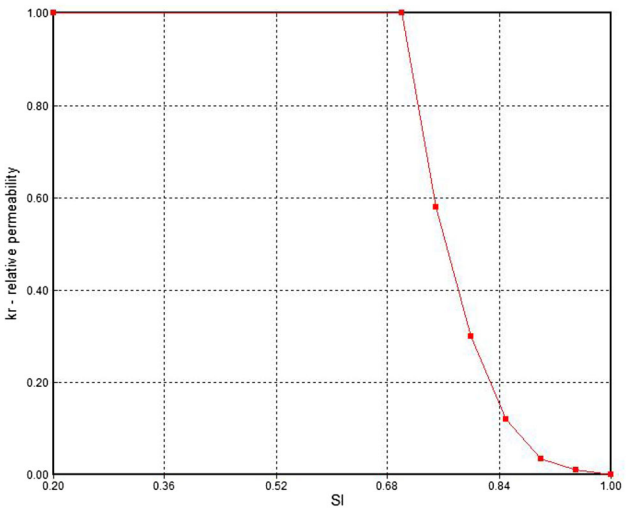

Fig. 14 Relative permeability versus saturation

more points in the actual considered reservoir. For instance, presently in the assumed reservoir matrix of $5 \times 5 \times 5$ order the numbers of values calculated are 125, but as we increase the order of matrix to $10 \times 10 \times 10$, the number of pressure values for given matrix will be 1000. Moreover, the same thing can be done with decreasing the time step values as discussed before (Fig. 18).

The following are the main inference and findings that are derived post-studying the pattern and the values of the pressure:

- The pressure values thus obtained from the code will be helpful in flow characterization.
- The major aim was to get the pressure-related values which will be placed in the simulation-based software like CMG and Ansys Fluent.
- The pressure values thus obtained are declined in correspondence to the software.
- As we can see from the coding outputs, the various pressure values which will be further utilized in obtaining the flowrate at specific predetermined points and hence the aim will be satisfied.
- These results are of extreme importance from the simulation point of view as they are the final building block of the flow characterization equation.
- The pressure drop can also be examined durationwise for any value of time interval, for example, finding the pressure drop at a fixed point from the given date to 10 days after or 20 days after as per the user requirement.
- The pressure drop pattern of the complete reservoir can be monitored.
- It is seen that more pressure drop is occurring at the boundaries than compared to the inner layers of the reservoir matrix.
- The values obtained can be further filtered for getting the pressure values at boundaries.
- The code is an intensive code which can be inherited for further usage to find the pressure values of each block formed by the creation of the fractures.

Results by CMG-IMEX simulator

In this, after the preparation of model the model was validated using the CMG-IMEX; now after the basic step of validation at present these values were obtained and the launch window was obtained in which results could be obtained in the following ways:

Graphical form

In this, the various graphs were obtained in the model for the water cut and gas production scenario these are attached and explained accordingly (Fig. 19).

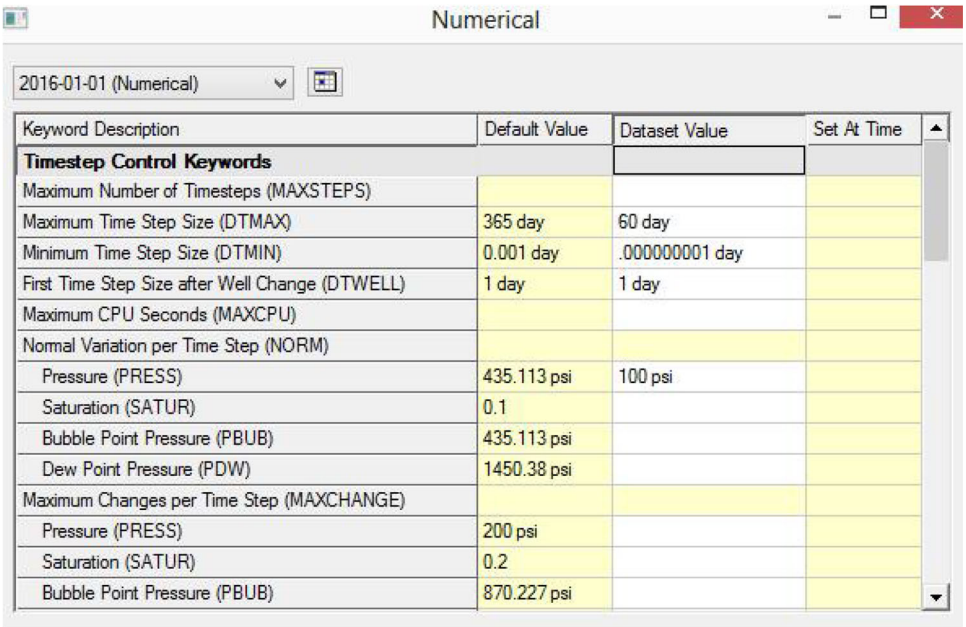

Fig. 15 Input of numerical values

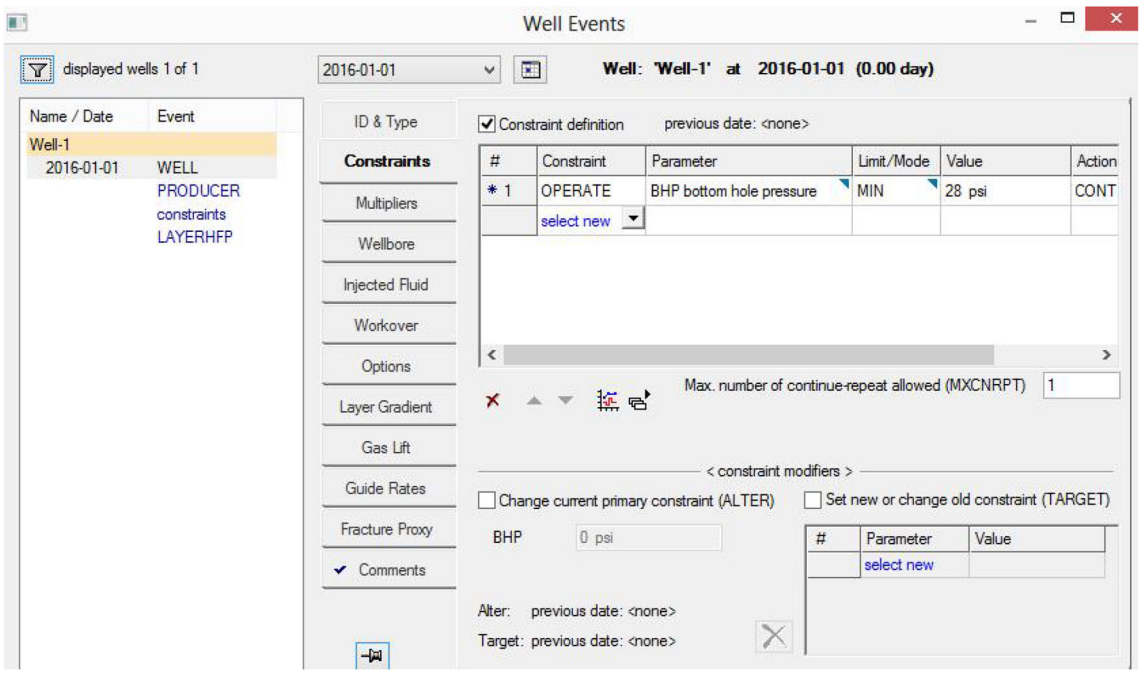

Fig. 16 Well conditions

The above resultant graph explains about the cumulative gas output from our well in the yearly basis. This graph also represents the yearly and monthly output of the gas from the shale reservoir with the values that can be obtained at every position in reservoir and any point of time (Fig. 20).

This graph is very important from result point of view as this contains the essence of the project and the pressure value declining with respect to time is thus obtained in the well. The pressure values are obtained for the well block which originally contained the gas, and hence, these values decline over a period of 10 years which shows the daily depletion rate. The pressure decline is constant as there is no aquifer support that was used and only the decline was considered on the initial pressure.

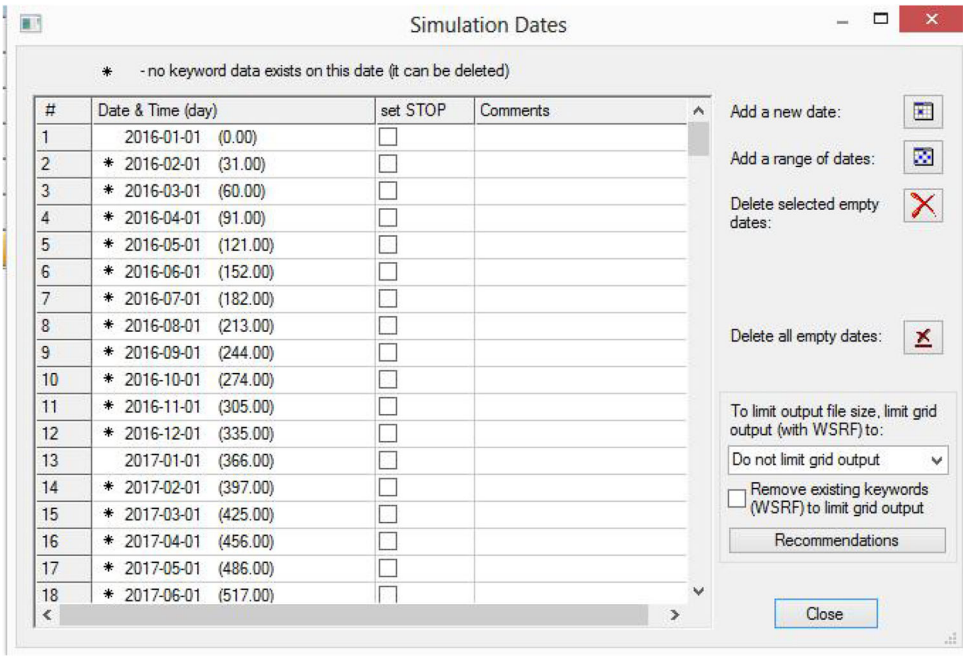

Fig. 17 Date selection

3-D form

In 3-D, the pressure transient model was developed and all the files are present in the compact drive which can be run through the CMG-IMEX simulator present (Fig. 21).

The primary fracture was also induced by the step of initially selecting dual-porosity model. The secondary is induced by two ways.

- Linear grid refinement.
- Applying in well constraint.

This is an actual model of the field data which is for the basic representation of the pressure dropping the field with respect to time and also shows the change in pressure with respect to fracture. The final change in fracture pressure is at much higher rate than normal due to an induced special permeability zones. In this, the special kind of conductivity is defined by inducing the changed permeability values and by the task of changing conductivity the secondary fracture is assumed.

Validation

In this section, the results obtained by MATLAB and CMG-IMEX simulator had been compared to check the perfection of the developed new dual-porosity model (Fig. 22).

Conclusion

In this work, we have presented an updated dual-mechanism dual-porosity formulation for a fractured shale gas reservoir. It has been concluded that the role of natural fractures in gas production from shale reservoirs can be ignored. As the obtained results state the flow rates of gas into the horizontal wellbore are almost the same. Modeling and simulation of gas flow behavior in shale gas reservoirs show the applicability in the real-life projects where it is difficult to model the fractures and also to obtain the flow rate in the fractures.

Fig. 18 Sample pressure values

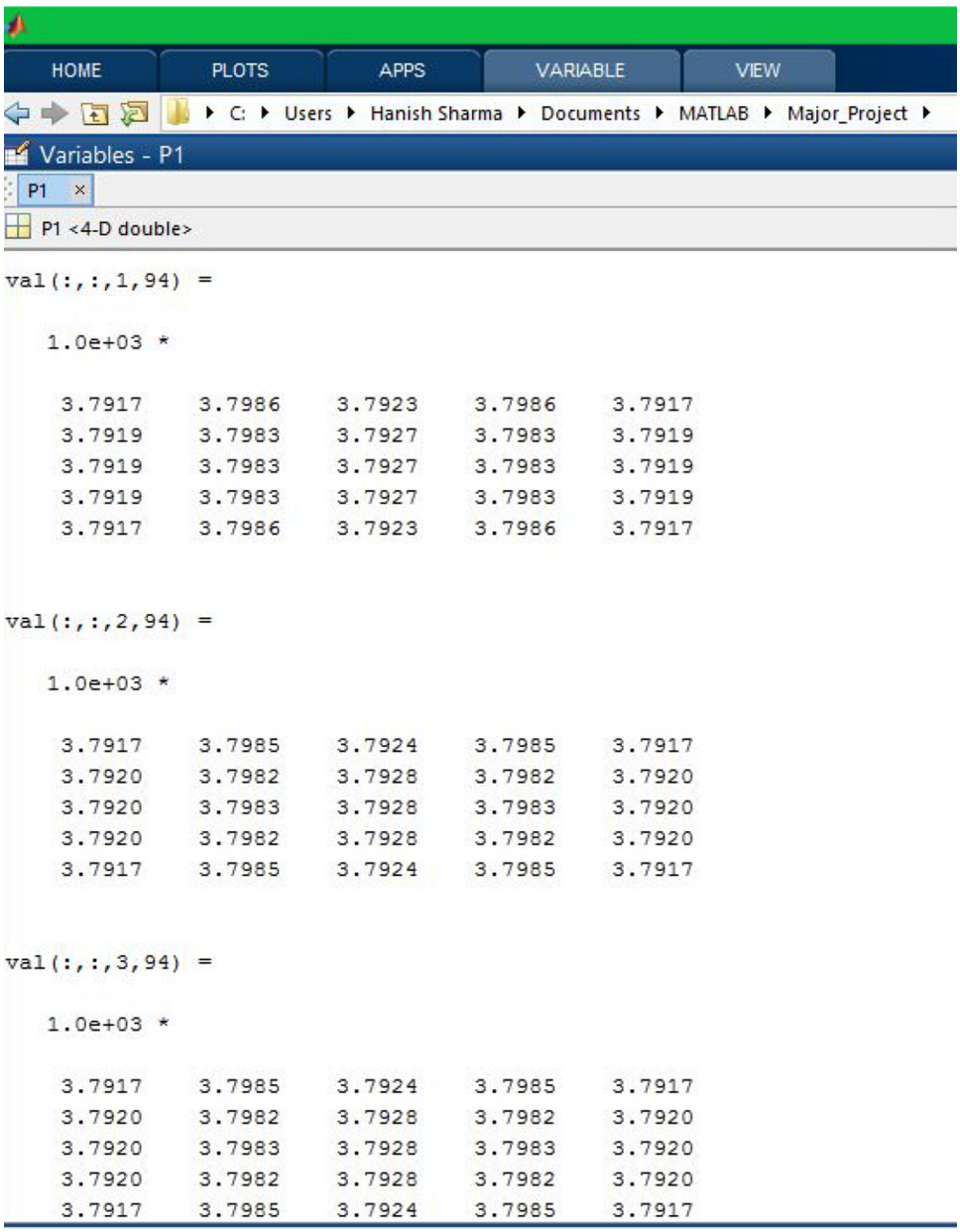

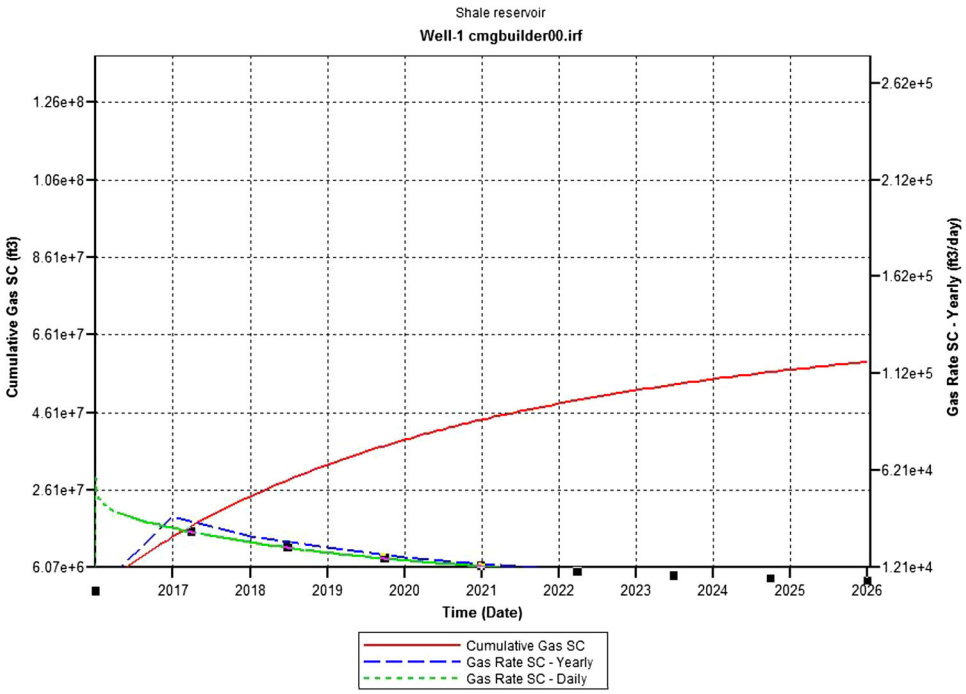

Fig. 19 Cumulative gas production versus time

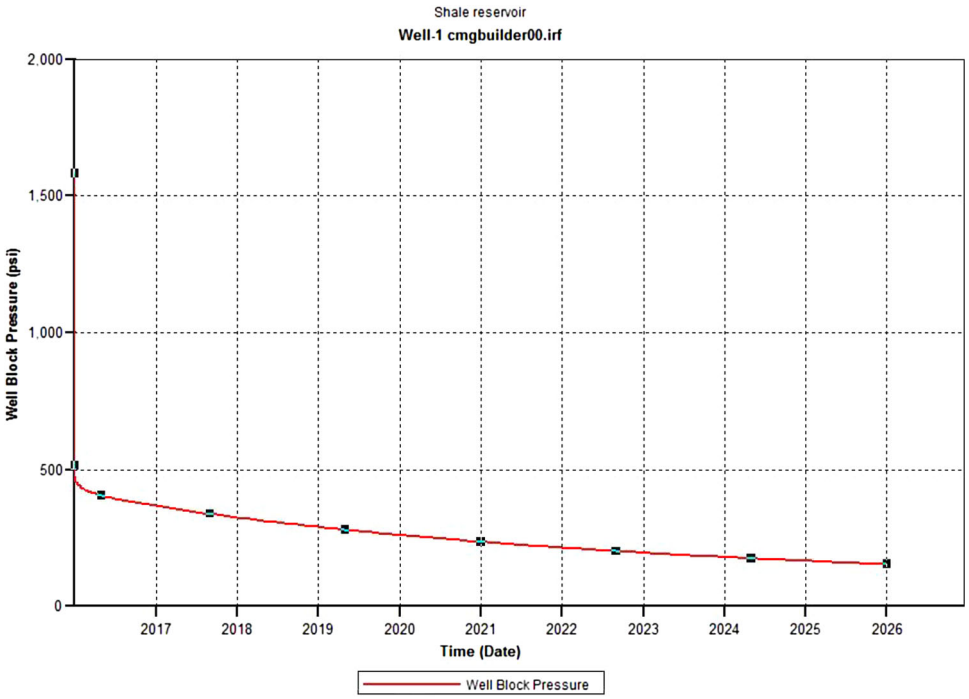

Fig. 20 Well block pressure versus time

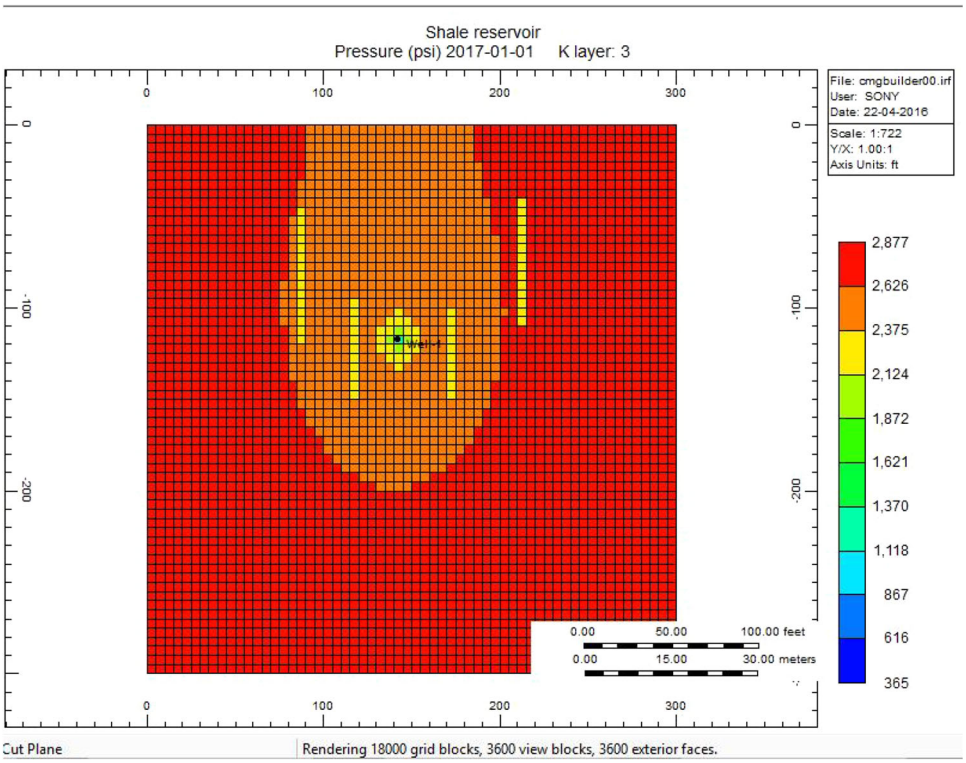

Fig. 21 3-D dynamic pressure depletion

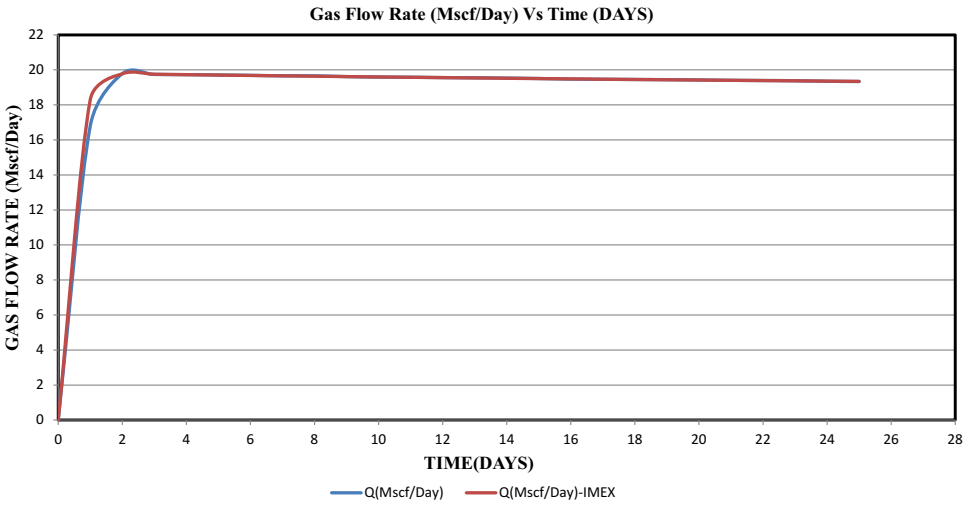

Fig. 22 Variation of flow rate (Mscf/Day) versus time (DAYS)

Acknowledgements Authors are extremely thankful to Dr. Kamal Bansal, Dean, COES, UPES, Dehradun for providing the valuable support whenever required.

Appendix 1: Complete MATLAB program for the calculation of pressure values of 3-D matrix

```
clc
close all
clear all

Pm = 3800;  % Initial Reservoir Pressure

% length of block
dx = 22;
dy = 12;
dz = 2;

dt = 10;    % Time Interval

T = 1000;   % Total days

n = 5;      % no. of matrix

i=1;
j=1;
k=1;

Ax=dy*dz;
Ay=dx*dz;
Az=dx*dy;
B(n,n,n) = 0;
S(n,n,n) = 0;
W(n,n,n) = 0;
E(n,n,n) = 0;
N(n,n,n) = 0;
A(n,n,n) = 0;
X(n,n,n) = 0;

m=T/dt;
P(n,n,n,m) = 0;
dP(n,n,n) = 0;

Km = klinkenberg(Pm);
Tgsc= trans(Pm);
Sgm=1;

B(:,:,:)= (Km * Az*Tgsc)/dz;
S(:,:,:)= (Km * Ay*Tgsc)/dy;
W(:,:,:)= (Km * Ax*Tgsc)/dx;
E(:,:,:)= (Km * Ax*Tgsc)/dx;
N(:,:,:)= (Km * Ay*Tgsc)/dy;
A(:,:,:)= (Km * Az*Tgsc)/dz;
X(:,:,:)= ((-
1)*(dx*dy*dz)/dt)*((Sgm*mat_por(Pm)*cmprs(Pm)
*rho_sc()/(5.61458*Bg_factor(Pm)))+(
mat_por(Pm)*cmprs(Pm)*(ad_vol(Pm)+de_vol(Pm))));
Q = -1*X*Pm;
C = (E+W+N+S+A+B-X);

tun(125,125)=0;
lun(125,1)=0;

for y=1:int16(fix((T/dt)))

for x=1:125

   [i,j,k]=index(x);

   lun(x,1)=Q(i,j,k);

   temp=(25*(i-1))+(5*(j-1))+k;
   tun(x,temp)= C(i,j,k);

   i1 = i-1;
   if i1>=1
   temp=(25*(i1-1))+(5*(j-1))+k;
   tun(x,temp)=W(i,j,k);
   end

   j1 = j-1;
   if j1>=1
   temp=(25*(i-1))+(5*(j1-1))+k;
   tun(x,temp)=S(i,j,k);
   end

   k1 = k-1;
   if k1>=1
   temp=(25*(i-1))+(5*(j-1))+k1;
   tun(x,temp)=B(i,j,k);
   end

   i1=i+1;
   if i1<=5
   temp=(25*(i1-1))+(5*(j-1))+k;
   tun(x,temp)=E(i,j,k);
   end

   j1=j+1;
   if j1<=5
   temp=(25*(i-1))+(5*(j1-1))+k;
   tun(x,temp)=N(i,j,k);
   end

   k1=k+1;
   if k1<=5
   temp=(25*(i-1))+(5*(j-1))+k1;
   tun(x,temp)=A(i,j,k);
   end

end

sol=tun\lun;

for x=1:125
   [i,j,k]=index(x);
   dP(i,j,k)=sol(x);
end
```

```
for i=1:n
   for j=1:n
      for k=1:n
         if y==1
            P(i,j,k,y)= Pm - dP(i,j,k);
         else
            P(i,j,k,y)= P(i,j,k,y-1)- dP(i,j,k);
         end
      end
   end
end

for i=1:n
for j=1:n
for k=1:n

   Km=klinkenberg( P(i,j,k,y) );
   Tgsc = trans( P(i,j,k,y) );

   B(i,j,k)= (Km * Az*Tgsc)/dz;
   S(i,j,k)= (Km * Ay*Tgsc)/dy;
   W(i,j,k)= (Km * Ax*Tgsc)/dx;
   E(i,j,k)= (Km * Ax*Tgsc)/dx;
   N(i,j,k)= (Km * Ay*Tgsc)/dy;
   A(i,j,k)= (Km * Az*Tgsc)/dz;

        X(i,j,k)= ((-
        1)*(dx*dy*dz)/dt)*((Sgm*mat_por(P(i,j,k,y))*cmprs(P(i,j,k,y))*rho_sc()/(5.61458
        *Bg_factor(P(i,j,k,y))))+(mat_por(P(i,j,k,y))*cmprs(P(i,j,k,y))*(ad_vol(P(i,j,k,y))+
        de_vol(P(i,j,k,y)))));
   Q(i,j,k) = -1*X(i,j,k)*P(i,j,k,y);
        C(i,j,k) = (E(i,j,k)+W(i,j,k)+N(i,j,k)+S(i,j,k)+A(i,j,k)+B(i,j,k)-X(i,j,k));

end
end
   end

end

P1(n,n,n,m)=0;

for y=1:m
   for i=1:n
      for j=1:n
         for k=1:n
            P1(i,j,k,y)=P(k,i,j,y);
         end
      end
   end
end
```

Appendix 2: Complete MATLAB code for the function viscosity()

```
function [ u_g ] = viscosity( Pm )
% viscosity() calculates viscosity of the gas at given reservoir
% temperature and pressure.
M_air=28.96;
spgr=Avg_Mol_Wt()/M_air;

T=660;  %Reservoir Temperature= 660 deg R (Literature)

u_uncorrected = ((1.709 * (10^(-5)-(2.062*10^(-6)*spgr)))*(T-460))+((8.118*10^(-3))-
(6.15*10^(-3)*log10(spgr)));

yCO2 = 0.03;
yN2 = 0.02;
yH2S = 0.01;
u_CO2 = (yCO2*(((9.08*10^(-3))*(log10(spgr)))+ (6.24*10^(-3))));
u_N2 = (yN2*((8.48*10^(-3)*log10(spgr))+ (9.59*10^(-3))));
u_H2S = (yH2S*((8.49*10^(-3)*log10(spgr))+ (3.73*10^(-3))));

u1 = u_uncorrected + u_CO2 + u_N2 + u_H2S ;

Tpc = 168 + (325 * spgr) - (12.5*(spgr^2));
Ppc = 677 + (15*spgr) - (37.5*(spgr^2));
Tpr = T/Tpc;
Ppr = Pm/Ppc;
% Constants for viscosity relation
a0 = -2.4621182;
a1 = 2.970547414;
a2 = -0.286264054;
a3 = 0.008054205;
a4 = 2.80860949;
a5 = -3.49803305;
a6 = 0.36037302;
a7 = -0.01044324;
a8 = -0.793385648;
a9 = 1.39643306;
a10 = -0.149144925;
a11 = 0.004410155;
a12 = 0.083938718;
a13 = -0.186408848;
a14 = 0.020336788;
a15 = -0.000609579;

syms ug;
con = a0+(a1*Ppr)+(a2*(Ppr^2))+ (a3*(Ppr^3))
+((Tpr)*(a4+(a5*Ppr)+(a6*Ppr^2)+(a7*Ppr^3)))+((Tpr^2)*(a8+(a9*Ppr)+(a10*Ppr^2)+(a11
*Ppr^3)))+((Tpr^3)*(a12+(a13*Ppr)+(a14*Ppr^2)+(a15*Ppr^3)));
eqn = ((Tpr*ug) == u1*exp(con) );
temp = solve(eqn,'ug');
u_g = double(temp);

end
```

References

Alahmadi HAS (2010) A triple-porosity model for fractured horizontal wells. Texas A&M University, College Station

Behar F, Vandenbroucke M (1987) Chemical modelling of kerogens. Org Geochem 11:15–24

Brown M, Ozkan E, Raghavan R, Kazemi H (2009) Practical solutions for pressure transient responses of fractured horizontal wells in unconventional reservoirs. SPE 125043

Bustin RM, Bustin AMM, Cui X, Ross DJK, Pathi VSM (2008) Impact of shale properties on pore structure and storage characteristics. Paper SPE 119892, presented at the 2008 SPE shale gas production conference, Ft. Worth, TX, USA, 16–18 November

Civan F, Rai CS, Sondergeld CH (2011) Shale permeability determined by simultaneous analysis of multiple pressure-pulse measurements obtained under different conditions. Paper presented at the SPE North American Unconventional Gas Conference, Woodlands, Texas, USA, 14–16 June 2011

Clarkson CR, Nobakht M (2011) Analysis of production data in shale gas reservoirs: rigorous corrections for fluid and flow properties. SPE 149404

Clarkson C, Williams J (2012b) Using production data to generate P10, P50 and P90 forecasts for shale gas prospect Analysis. SPE 162711

Clarkson CR, Nobakht M, Kaviani D (2012a) New and improved methods for performing rate-transient analysis of shale gas reservoirs. SPE 147869

Dahaghi AK, Mohaghegh SD (2011) Numerical simulation and multiple realizations for sensitivity study of shale gas reservoirs. SPE 141058

Dahaghi AK, Mohaghegh SD, Khazaeni Y (2010) New insight into integrated reservoir management using top-down, intelligent reservoir modeling technique: application to a giant and complex oil field in the middle east. SPE 132621

Daniel Arthur J, Coughlin Bobbi Jo (2012) Hydraulic fracturing considerations for natural gas wells of the Fayetteville shale. School of Energy, China University of Geosciences, Beijing

Ding W, Li C, Li C, Xu C, Jiu K, Zeng W, Wu L (2011) Fracture development in shale and its relationship to gas accumulation. J Geosci Front 3(1):97–105

Dreier J (2004) Pressure transient analysis of wells in reservoirs with a multiple fracture network. Colorado School of Mines, Golden

Fathi E, Akkutlu IY (2012) Lattice boltzmann method for simulation of shale gas transport in kerogen. SPE 146821

Firoozabadi A (2012) Nano-particles and nano-pores in hydrocarbon energy production. Research talk delivered at University of Calgary, December 7

Gong B, Qin G, L Bi, X Wu (2011) Multiscale and multi physics methods for numerical modeling of fluid flow in fractured formations. SPE 143590. SPE EUROPEC annual technical conference and exhibition, Vienna, Austria, USA, 23-26 May

Hong L, Zeng F, Yao S (2013) A semi analytical model for hydraulically fractured wells with stress sensitive conductivities. SPE 167230

Javadpour F (2009) Nanopores and apparent permeability of gas flow in mudrocks (shales and siltstones). J Can Pet Technol 48(48):16–21

Javadpour F, Fisher D, Unsworth M (2007a) Nanoscale gas flow in shale gas sediments. J Can Pet Technol 46(10):55–61

Javadpour F, Fisher D, Unsworth M (2007b) Nanoscale gas flow in shale gas sediments. J Can Pet Technol 46(10):55–61

Michel L, Flynn MJ, Hoo CH (2011) Application of PSDM imaging for reservoir characterization in the Northern Malay Basin: a case study. SPE 14817

Ozkan E, Raghavan R, Aypadin O (2010) Modeling of fluid transfer from shale matrix to fracture network. Paper SPE 134830 presented at the SPE annual technical conference and exhibition held in Florence, Italy, 19–22 September

Rushing JA, Oliver SJP, Scheper RJ (1989) Reservoir simulation of the antrim shale in the Michigan basin. SPE 19313

Sakhaee-Pour A, Bryant S (2012) Gas permeability of shale. SPE 146944

Schepers KC, Gonzalez RJ, Koperna GJ, Oudinot AY (2009) Reservoir modeling in support of shale gas exploration. Paper SPE 123057, presented at 2009 SPE Latin American and caribbean petroleum engineering conference, Cartagena, Colombia, 31 May–3 June 2009

Song B, Ehlig-Economides CA (2011) Rate normalized pressure analysis for determination of shale gas performance. SPE 144031. SPE North American unconventional gas conference and exhibition, 14–16 June, The Woodlands, Texas, USA

Song C, Yang D (2013) Performance evaluation of CO2 huff-n-puff processes in tight oil formations. Paper SPE 167217, SPE unconventional resources conference, Alberta, Canada, 5–7 November

Swami V, Clarkson CR, Settari A (2012) Non-darcy flow in swami, Vivek. 2012. Shale gas reservoir modeling: from nano pores in laboratory. SPE 163065

Swami V, Settari A, Aguilera R (2013) Modeling of stress dependent permeability tensor with pressure depletion/injection for fractured reservoirs. SPE-164839-MS, to be presented at 2013 SPE EUROPEC in London, UK. doi:10.2118/164839-MS

Wang FP, Reed RM (2009) Pore networks and fluid flow in gas shales. Paper SPE 124253, presented at the 2009 SPE annual technical conference and exhibition, New Orleans, LA, USA, 4–7 October

Zhang JG, Yuan ZW (2002) Forming conditions of oil and gas reservoirs in mudstone and its resources potential. J Oil Nat Gas Geol 23(4):336–338

Zuber MD, Williamson JR, Hill DG, Sawyer WK, Frantz Jr. JH (2002) A comprehensive reservoir evaluation of a shale reservoir—The New Albany Shale. Paper SPE 77469, presented at the 2002 SPE annual technical conference and exhibition, San Antonio, TX, USA, 29 September–2 October